sustainability

MDPI

Article

A Study of the Physical and Mechanical Properties of Yellow River Sediments and Their Impact on the Reclamation of Coal-Mined Subsided Land

Huang Sun [1], Zhenqi Hu [1,2,*] and Shuai Wang [1]

[1] College of Geosciences and Surveying Engineering, China University of Mining and Technology-Beijing, Beijing 100083, China; sunhuang@student.cumtb.edu.cn (H.S.); sqt2100204086@student.cumtb.edu.cn (S.W.)
[2] School of Environment and Spatial Informatics, China University of Mining and Technology, Xuzhou 221116, China
* Correspondence: huzq@cumtb.edu.cn; Tel.: +86-139-1063-7448

Abstract: Coal mining in China has resulted in numerous subsided areas, exacerbating land scarcity issues. The Yellow River carries a high sediment load of nearly 1.6 billion tons annually. Cleaning up the accumulated silt is costly and takes up land. Reusing the sediment from the Yellow River to fill and reclaim the subsided areas caused by coal mining addresses both sedimentation and land reclamation issues, killing two birds with one stone. Nonetheless, technical challenges have emerged, such as machinery sinking into the soil, difficulty draining water, and poor soil quality improvement. To tackle these issues, understanding the physical and mechanical properties of Yellow River sediment is essential. Results show that the average particle size (D_{50}) is 0.08 mm, categorized as fine-grained sandy soil with a relatively uniform particle size distribution. The permeability coefficient is 2.91×10^{-3} cm·s^{-1}, similar to that of silty soil, indicating the feasibility for filling reclamation. However, the low permeability requires drainage improvement to accelerate construction timelines. The internal friction angle of the sediment ranges from 34.67° to 31.76°, with a cohesion from 20.79 to 23.92 kPa. To ensure safe and stable construction, machinery must not sink into the fill material. It is recommended to enhance drainage to about 13% for quicker drainage and stable construction. The sediment has a compression coefficient of 0.05 MPa^{-1}, indicating low compressibility. Mechanical compression is not economically viable during the reclamation process. Design elevation (H) and fill elevation (h) should account for cumulative deformation settlement.

Keywords: Yellow River sediment; coal-mined subsided land; physical and mechanical properties; filling reclamation; engineering construction

check for updates

Citation: Sun, H.; Hu, Z.; Wang, S. A Study of the Physical and Mechanical Properties of Yellow River Sediments and Their Impact on the Reclamation of Coal-Mined Subsided Land. *Sustainability* **2024**, *16*, 439. https://doi.org/10.3390/su16010439

Academic Editor: Rajesh Kumar Jyothi

Received: 19 October 2023
Revised: 26 December 2023
Accepted: 27 December 2023
Published: 4 January 2024

1. Introduction

Coal plays an essential role in China's energy mix, accounting for 57.14% of total consumption according to the National Bureau of Statistics over the past 5 years, and the average coal consumption was 5.026 billion tons. While supporting the development of the national economy, coal mining also causes significant land damage from excavation, subsidence, and occupation, which significantly impacts the ecological environment of mining areas [1–3]. Coal mining subsidence has caused irreversible damage to arable land [4,5], exacerbating the already strained situation of insufficient per capita cultivated land resources. Therefore, China has begun to pay attention to land reclamation and ecological restoration in mining areas in the past 30 years, and local governments and coal enterprises have invested heavily in implementing a series of land reclamation and ecological restoration projects in mining areas. The aim is to address the damage caused by excavation and subsidence.

However, a significant limiting factor in reclaiming coal-mined damaged land through reclamation is the scarcity of suitable filling materials. Fly ash [6,7] and coal gangue [8] have commonly been used as filling materials for reclamation due to their availability, but the limited quantity and potential pollution of fly ash and coal gangue [8–10] are major concerns. Fly ash, due to its alkalinity, high salinity, and cementitious ability, harms plant growth [11]. In addition, the porous structure of filling materials such as coal gangue and fly ash results in insufficient water retention, hindering the upward movement of water in the lower layers [12], which restricts the application of this technology.

Yellow River sediment, as a significant hazard, causes blockages in the river channels [13], and the dredging of sediment deposits occupies a large amount of land [14]. However, Yellow River sediment can be used as a pollution-free filling material for reclamation [15], especially the fine-grained deposits in the main channel. The use of Yellow River sediment for reclamation can solve the problem of dredging sediment and reclaim a large amount of land damaged by coal mining along the Yellow River, killing two birds with one stone. This approach has successfully reclaimed substantial subsided areas [16]. Transported through pipelines, accumulated Yellow River sediment reduces land occupation and surface impacts during transportation [17], ensuring efficient transportation. The transported sediment contains a certain amount of water, and the wet sediment requires draining from the sediment-filled coal-subsided area before further reclamation, such as turning it into arable land. Nevertheless, drainage is challenging as the wet sediment settles slowly after filling through pipelines, and the overflow risks field waterlogging and blockages [18]. Additionally, long filling strips make stagnant water challenging to drain, with the liquefaction potential and the stagnant water of sediment remaining even after half a year of drainage during construction (Figure 1d) [17]. Secondly, the water-holding capacity of Yellow River sediment is not as good as that of the original soil, as it mainly consists of fine particles. Therefore, soil reconstruction is also essential during the reclamation process. Understanding the physical and mechanical properties of Yellow River sediment is crucial for providing theoretical support for the filling reclamation of coal-subsided areas and accumulating experience in engineering practices. This will guide the large-scale application of Yellow River sediment in improving the ecological environment from an environmental protection perspective and achieving green and sustainable development.

The utilization of Yellow River sediment resources can be broadly categorized into two main approaches. One category is to use sediment as the aggregate for building materials, such as roadbed materials. Research shows Yellow River sediment belongs to well-graded sandy soil in the intermediate range of highway soil, with a maximum dry density range of 1.62~1.65 $g \cdot cm^{-3}$, indicating that it is feasible to use Yellow River sediment for high-speed highway roadbed filling materials [19]. However, Yellow River sediment naturally exhibits some disadvantages like relatively low strength and dispersiveness due to its soil properties [20]; by adding $Ca(OH)_2$ through alkali activation, the compressive strength of specimens can be significantly improved [21]. In addition, using Yellow River sediment to prepare alkali-activated fly ash (AAFA) foam concrete, and incorporating the AAFA as a supplementary binder material, can significantly improve the mechanical properties [22,23]. This approach effectively addresses the inherent weaknesses of the sediment by chemically modifying its makeup. The other primary utilization involves the application of Yellow River sediment in reclamation. Research shows that Yellow River sediment is pollution-free and can be used as a filling material for reclamation [15], especially the fine-grained sediment in the main channel. Even the Yellow River sediment can be used as a soil amendment for the amelioration of saline land in the Yellow River Delta [24]. However, issues arise during filling reclamation. Water and nutrient leakage from the sediment layer can affect the quality of the reclaimed soil [16]. Studies on reclamation have found that the sediment layer lacks adequate water-holding capacity, posing obstacles to the productivity of reclaimed soil [25]. To address this, Zhenqi Hu [26] proposed a "sandwich-structure" method for the filling reclamation of soil using Yellow River sediment. Further research on multiple profiles have shown that this approach can effectively reduce water seepage when used for reclamation [27]. The sandwich design better retains water by enclosing sediment layers between more conducive materials.

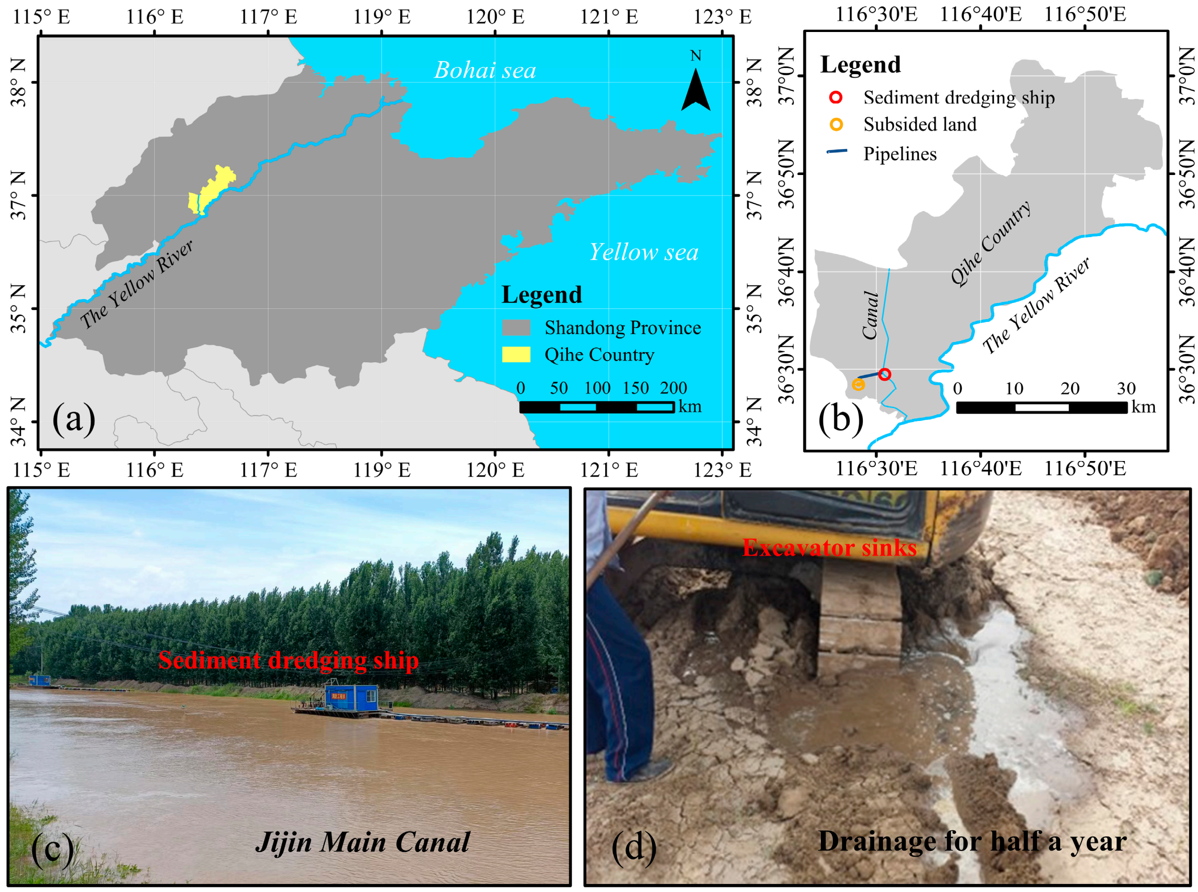

Figure 1. (**a**) Location of the study area; (**b**)Reclamation of coal-mined subsided land by desilting sediments from Jijin Main canal. (**c**) Jijin Main Canal and the sediment dredging ship; (**d**) Mechanical sinking and water rising for half a year after the drainage of the backfilled subsided land.

The physical and mechanical properties of sediment in the Yellow River undoubtedly influence the strength of reconstructed soils. Therefore, various factors must be considered during the soil reconstruction to ensure high-quality reclamation, including soil permeability, water retention, and compressive strength under construction loads. These considerations will help ensure the high-quality reclamation of filling reclamation land. However, current research on the filling reclamation coal-mined subsided land with Yellow River sediment has not sufficiently examined these essential soil properties and phenomena. A lack of understanding in how unique sediment characteristics influence reclamation outcomes poses risks to engineering design and long-term land sustainability goals.

This study aims to address the following issues: (1) Analyzing the physical and mechanical properties of Yellow River sediment and evaluating its suitability for filling reclamation. (2) Investigating the impact of the physical and mechanical properties of Yellow River sediment on drainage obstacles and drainage standards during the construction process of reclamation projects. (3) Exploring the impact of the physical and mechanical properties of Yellow River sediment on filling elevation and construction standards during the construction process of reclamation projects.

2. Materials and Methods

2.1. Experimental Materials

Yellow River sediment was obtained for this study from dredging operations at the Yellow River Jijin Main Canal in Jining County, Dezhou City, Shandong Province (Figure 1). Over 3000 acres of coal-mined subsided land have been reclaimed using sediment from this site transported by pipelines. The sediment used in experiments was collected from the Yellow River Jijin Main Canal by the sediment dredging ship. A total of 31 sediment samples were collected from the sediment transfer point and the filling reclamation land by three sediment dredging ships in the main canal. After removal of impurities, the sediments were used as test materials. Experimental water with a pH of 7.64 and conductivity of 696 uS·cm^{-1} was employed to closely mimic field conditions. Previous research recommended a filling height of approximately 120 cm for Yellow River sediment reclamation [17]. As the retrieved Yellow River sediment is a disturbed specimen, laboratory simulation filling experiments were conducted by filling PVC pipes with a concentration of 300 kg·m^{-3} of Yellow River sediment up to a height of 120 cm [17]. After 12 h of drainage, samples were taken at the top layer (0–40 cm), the middle layer (40–80 cm), and the bottom layer (80–120 cm) using a cutting ring, and their dry bulk density was determined after drying to constant weight.

2.2. Physical and Mechanical Properties Determination Method

(1) Relative density

According to the requirements of the Geotechnical Test Procedure GB-T50123-2019 [28], the volumetric method was used to conduct the minimum dry density test for relative density. A representative and sufficiently air-dried specimen of Yellow River sediment (m_d) was uniformly poured into a funnel. The funnel and plunger were then raised simultaneously, and then the plunger was lowered to detach the cone from the funnel mouth. This allows the specimen to fall slowly and evenly into the graduated cylinder. After the specimen had completely entered the graduated cylinder, the funnel and conical plug were removed, and the sediment surface was levelled using a sediment levelling tool without causing any vibration to the cylinder. The volume (V_{max}) of the sand specimen was then measured, and the minimum dry density (ρ_{dmin}) was calculated.

$$\rho_{dmin}\left(\mathrm{g}\cdot\mathrm{cm}^{-3}\right) = \frac{m_d}{V_{max}} \quad (1)$$

According to the requirements of the Geotechnical Test Procedure GB-T50123-2019, the maximum dry density was determined by the vibratory hammer method. A representative specimen (m_d) was poured into a 1000 mL container. The container was then struck on both sides using a vibrating fork at a frequency of 150 times per minute and, simultaneously, a hammer was used to strike the surface of the sample at a rate of 30 times per minute until the volume of the sand sample (V_{min}) no longer changed. Finally, the maximum dry density (ρ_{dmax}) was calculated as

$$\rho_{dmax}\left(\mathrm{g}\cdot\mathrm{cm}^{-3}\right) = \frac{m_d}{V_{min}} \quad (2)$$

using the specific gravity method to determine the specific gravity of the specimen.

$$G_s\left(\mathrm{g}\cdot\mathrm{cm}^{-3}\right) = \frac{m_d}{m_{bw} + m_d - m_{bws}} G_{wT} \quad (3)$$

where m_{bw} is the total mass of specific gravity bottle and water (g); m_{bws} is the total mass of specific gravity bottle, water, and dry soil (g); G_{wT} is the specific gravity of pure water at T °C.

According to the national industry standard NYT 1121.4-2006 [29], the dry bulk density of sediment profiles can be determined. To do so, select a remolding sediment profile and use a cutting ring to cut specimens from the top down, corresponding to the soil profile layers. The cutting ring, filled with the soil specimen, is then placed directly in a constant temperature drying oven at 105 °C ± 2 °C until a constant weight is achieved. The specimen is then weighed and measured using a balance with an accuracy of one percent.

$$\mathrm{BD}\left(\mathrm{g}\cdot\mathrm{cm}^{-3}\right) = \frac{m_1 - m_2}{V} \tag{4}$$

where BD is the soil bulk weight ($\mathrm{g}\cdot\mathrm{cm}^{-3}$); m_1 is the mass of the ring knife and the dried constant weight dry soil (g); m_2 is the mass of the dried constant weight ring knife (g) and V is the volume of the ring knife (cm^{-3}).

Sediment particles were measured by pipette method according to China water industry standard SL 42-2010 [30]. Based on Stokes' Law, a certain amount of suspended liquid specimen was slowly extracted at a particular depth using a transfer pipette at the moment when sedimentation began. After drying and weighing the specimen, the cumulative amount smaller than the corresponding particle size was calculated. The difference between the two cumulative measurements represented the amount of soil particles within a certain size range.

(2) Porosity and water content

The minimum water holding capacity of the Yellow River was calculated following the NY/T 1121.22-2010 [31] standard by remolding the sediment profile. Specimens were collected from top to bottom of the sediment profile using a cutting ring. The ring cut specimens were soaked in water for 4 h to achieve saturation. The saturated specimens were then placed in a sand bath within an enclosed container to prevent water evaporation. The mass of the ring cutter and wet specimen was measured and recorded every 2 h. Once a consistent mass was obtained, indicating complete saturation, the volume was recorded. The minimum water holding capacity was then calculated based on the weight of the saturated sediment specimen.

$$W_m(\%) = \frac{m_4 - m_2}{m_2 - m_0} \times 100\% \tag{5}$$

where $W_m(\%)$ is the minimum water holding capacity of the sediment (%); m_4 is the mass of dry sediment (g) of the ring knife with wet sediment placed semi-enclosed in the water bath chamber until constant weight; m_2 is the mass of the ring knife with dry sediment dried to constant weight (g); and m_0 is the mass of the ring knife after drying (g).

(3) Water permeability and plasticity

The permeability coefficient was determined according to the standard of Geotechnical Test Procedure GB-T50123-2019. A constant head permeameter TST-70 (Produced by Nanning Xicheng Soil Instruments Co., Ltd., Nanning, China) was used for the constant head permeability test. In the TST-70 constant head permeameter, the sediment with known water content was stratified and filled into the permeameter at a dry density of 1.6 $\mathrm{g}\cdot\mathrm{cm}^{-3}$. The sediment was then saturated from the bottom up using a water bottle. When water flows out from the outlet, the sediment is considered to be fully saturated. The water level above was kept stable, and the outlet was adjusted to positions at the upper, middle, and lower parts of the specimen to measure the water head height and outflow volume, respectively. The permeability coefficient was then calculated.

$$k_t\left(\mathrm{cm}\cdot\mathrm{s}^{-1}\right) = \frac{2QL}{At(H_1 + H_2)} \tag{6}$$

$$k_{20} = k_t \frac{\eta_T}{\eta_{20}} \tag{7}$$

where k_t is the permeability coefficient of the specimen at water temperature T °C ($\mathrm{cm}\cdot\mathrm{s}^{-1}$); Q time t seconds of permeable water volume cm^{-3}); L is the permeation length; A is the segment area of the specimen; t is the time; H_1, H_2 is the water level difference; k_{20} is the permeability coefficient of the specimen at standard temperature; η_T is the dynamic viscosity coefficient of water at T °C; η_{20} is the dynamic viscosity coefficient of water at 20 °C.

The limit water content was determined following the liquid limit and plastic limit joint determination method specified in Geotechnical Test Procedure GB-T50123-2019. First, 600 g of air-dried sediment was sieved through a 0.5 mm sieve and prepared for use. Specimens with different consistencies approximating the liquid limit, plastic limit, and intermediate state were prepared and left to pre-wet for 12 h, respectively. After the prepared specimen was compacted into the specimen cup, the depth of sinking of the 100 g cone penetrometer under its weight was measured using a liquid limit and plastic limit joint determination instrument. The relationship curve was plotted on logarithmic coordinates with water content as the abscissa and cone sinking depth as the ordinate. The water content corresponding to a sinking depth of 17 mm was taken as the liquid limit and the water content corresponding to a sinking depth of 2 mm was taken as the plastic limit. The plasticity index is the difference between the liquid limit and the plastic limit.

(4) Mechanical properties

The compaction characteristics were determined following the Geotechnical Test Procedure GB-T50123-2019. A ZJ strain-controlled direct shear apparatus (Nanjing Soil Instruments Factory Co., Ltd., Nanjing, China) was utilized to conduct the compaction test. A total of five 2000 g portions of air-dried sediment specimen were weighed and the water content was adjusted in increments of 2–3% of the optimum water content. This produced 5 graded wet sediment specimens, which were left to rest for 12 h. Each specimen was then compacted in 3 layers with 25 blows from a 2.5 kg light compaction hammer. The wet density after compaction was measured by weighing. Approximately 100 g of sample was taken from the center of each compacted specimen, dried, and the water content was determined. The dry density was then calculated.

The shear strength was determined following the Geotechnical Test Procedure GB-T50123-2019. A ZJ strain-controlled direct shear apparatus (Nanjing Soil Instruments Factory Co., Ltd.) was utilized to perform direct shear tests. Specimens with known unit weight were prepared using the compaction molding method based on the unit weight of the filled sediment and subjected to direct shear tests. The shear stress τ was calculated using the following equation.

$$\tau = CR \tag{8}$$

where τ is the shear stress, kPa; C is the force ring rate determination coefficient, N·0.01^{-1} mm; R is the percentage meter reading, 0.01 mm.

The deformations of test specimens obtained from compression tests is the most fundamental data for calculating indices such as porosity ratio, compression coefficient, compression modulus, and maximum drainage distance, and the results impact the design elevation of filling and reclamation construction of Yellow River sediment. Due to the fact that the pores of saturated filled Yellow River sediment are filled with water, the effective stress is low, and the bearing capacity of the soil body is diminished. In actual engineering practice, a certain amount of water must be drained before it can withstand the shear strength of construction machinery. Compression tests are carried out on samples with 17% water content and a dry density of 1.60 g·cm^{-3} to fully reflect the compression and consolidation of Yellow River sediment after drainage.

The compression characteristics were determined following the Geotechnical Test Procedure GB-T50123-2019. A TKA-STC-3L triple low-pressure consolidation instrument (Nanjing TKA Technology Co., Ltd., Nanjing, China) was utilized to conduct the consolidation test. Specimens with known unit weight were prepared using the compaction molding method based on the unit weight of the filled sediment and subjected to a quick consolidation test. The change in porosity was calculated from the deformation, and the compression curve was plotted. Calculate the compression coefficient a_v, compression index C_s and compression modulus E_s according to the following equations.

$$a_v = \frac{e_i - e_{i+1}}{p_{i+1} - p_i} \tag{9}$$

$$C_s = \frac{e_i - e_{i+1}}{\log p_{i+1} - \log p_i} \tag{10}$$

$$E_s = \frac{p_{i+1} - p_i}{(S_{i+1} - S_i)/1000} \tag{11}$$

where e_i, e_{i+1} is the porosity per unit pressure of i, i + 1; p_i, p_{i+1} is the vertical pressure at i, i + 1 unit pressure; S_i, S_{i+1} is the compressive deformation per unit pressure of i, i + 1.

2.3. Data Processing and Analasis

The mean and standard deviation of the sample results were first calculated, and then the standardized value (Z-score) of each result was calculated by subtracting the mean and dividing by the standard deviation. If the standardized value was greater than 3, the result was considered an outlier and was rejected. After removing the outliers, the means of the basic physical and mechanical properties were calculated to describe the basic characteristics of the test results. The precision of the mean values was statistically analyzed by calculating the precision of the mean values of the results of the test samples at a significance level of p = 0.05.

Boundary water content and Mohr's envelope were fitted linearly. Sediment grain size distribution curves were modelled using a curve equation model [32]:

$$P = \left(\left(\frac{d_*}{d}\right)^{\frac{m}{n}} + 1\right)^{-n} \tag{12}$$

where d is the sediment grain size, mm; d_* is the sediment grain size for the main trend, which is taken to be 0.1 mm in this study; P is the cumulative percentage less than a given sediment grain size (d), %; m is the slope of change in the central portion of the sediment grading curve in the double logarithmic coordinate system; and n is a transitional exponent.

Specimen data were analyzed and plotted using Origin 2021 graphing and data analysis software (OriginLab, Northampton, MA, USA).

3. Results

3.1. Physical Properties

3.1.1. Basic Physical Properties

As depicted in the figure below (Figure 2), the dry bulk density of the top layer (0–40 cm) was 1.58 g·cm^{-3}, the middle layer (40–80 cm) was 1.60 g·cm^{-3}, and the average dry bulk density of the bottom layer (80–120 cm) was 1.61 g·cm^{-3}. When all the pores were filled with water, the saturation density of the top layer (0–40 cm) was 1.99 g·cm^{-3}, the middle layer (40–80 cm) was 2.01 g·cm^{-3}, and the average saturation density of the bottom layer (80–120 cm) was 2.02 g·cm^{-3}.

In addition, the density of the specimen determined by the measuring cylinder method shows that the minimum dry density of the Yellow River sediment used for filling reclamation was 1.37 g·cm^{-3}. Meanwhile, the density of the specimen determined by the vibratory hammer method shows that the maximum dry density of the Yellow River sediment used for filling reclamation was 1.83 g·cm^{-3}. Finally, the specific gravity of the specimen was determined by the specific gravity method, which shows that the specific gravity of the Yellow River sediment used for filling reclamation was 2.696 $\pm$ 1.76% g·cm^{-3} (p = 0.05).

The particle size distribution of the Yellow River sediment used for filling reclamation was determined using the pipette method. The crimson fitted curve in the particle size distribution graph was predominantly situated to the right of the 0.5 mm dimension, denoting that the main particle size fraction of the sediment was below 0.5 mm. Furthermore, 100% of the particles exhibited diameters below 0.5 mm, affirming the relatively fine-grained nature of the reclamation sediment.

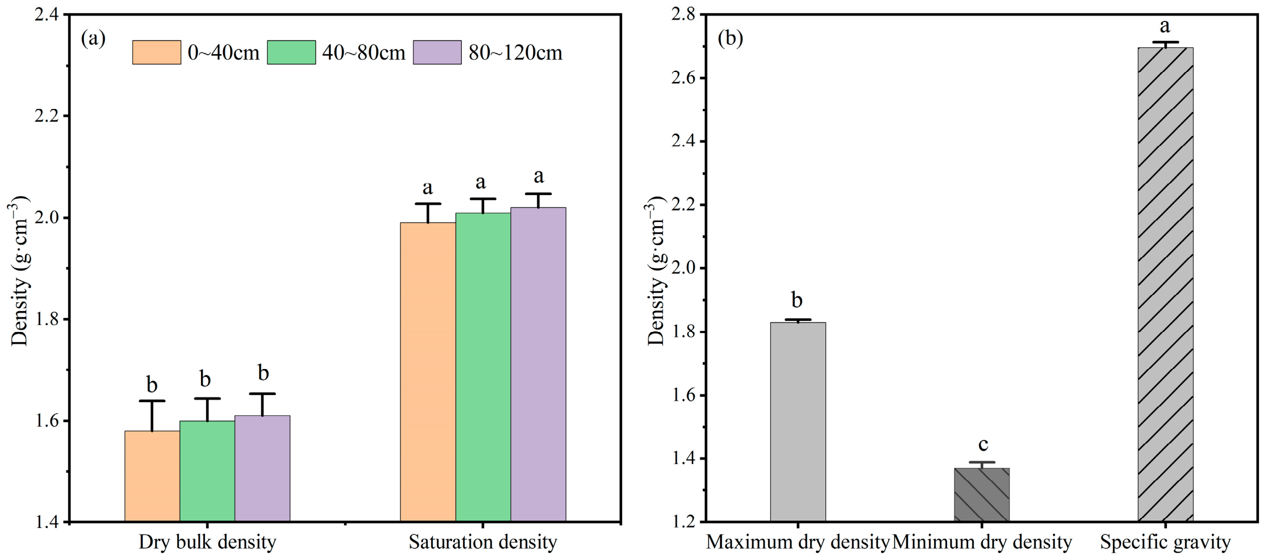

Figure 2. Basic physical properties of Yellow River sediment. (**a**) Dry bulk density and saturation density at different depths; (**b**) Maximum and minimum dry density and specific gravity.

The particle size of the filling reclamation Yellow River sediment measured was fitted (Figure 3), where m was the slope of the change in the middle section of the sediment grading curve in the double logarithmic coordinate system, and the fitted value was 2.269, which shows that the change in the middle section of the sediment was large. The value of n, the fitting coefficient, was 0.637. The fitted curve equation was $P = \left(\left(\frac{0.1}{d}\right)^{\frac{2.269}{0.637}} + 1\right)^{-0.637}$, and the value R^2 was 0.97, indicating a high fitting accuracy.

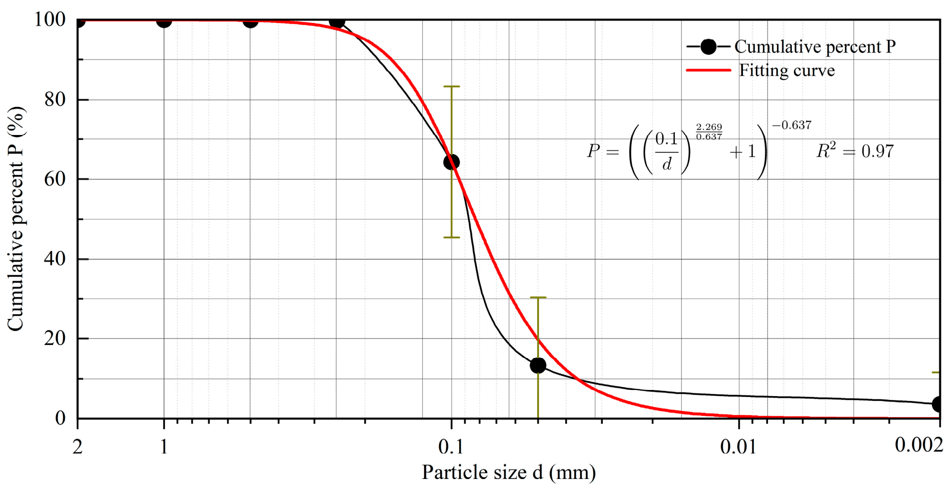

Figure 3. The particle size distribution curve of Yellow River sediment.

Based on the classification of fine-grained soil, the particle size distribution graph shows that the limit particle size (D_{60}) was 0.09 mm, the average particle size (D_{50}) was 0.08 mm, the intermediate particle size (D_{30}) was 0.07, and the effective particle size (D_{10}) was 0.04 mm. The coefficient of uniformity (C_u) was 1.75, which is close to 1. And the curvature coefficient (C_c) was 1.36, indicating a relatively uniform particle size distribution and poor grading. In general, the Yellow River sediment used for filling reclamation is classified as fine-grained sandy soil.

3.1.2. Porosity and Water Content

The void ratio of the Yellow River sediment used for filling and reclamation was 0.68, indicating that the volume of voids in the sediment is 0.68 times the volume of the solid particles. Correspondingly, the porosity was 40.64%, signifying the percentage of void space relative to the total volume.

The increased void ratio and porosity signify enhanced potential for settlement and deformation within the Yellow River sediment. This porous nature additionally governs permeability and drainage properties. Under the dry bulk density of 1.60 g·cm^{-3} obtained by the laboratory experimental method, the saturation capacity of the specimen was 40.64%, and the degree of saturation was 51.24%. This indicates that the Yellow River sediment can absorb a considerable amount of water when it is saturated. The minimum water holding capacity was 13.02%, which suggests that the Yellow River sediment can maintain a certain level of water content under natural conditions.

3.1.3. Water Permeability and Plasticity

In the constant head permeability test (Table 1), the measured permeability coefficient for the Yellow River sediment was 2.91 × 10^{-3} cm·s^{-1}, denoting a slow permeability rate. This indicates that the sediment has a slow permeability rate, which is much lower than that of coarse sand (6 × 10^{-1} cm·s^{-1}), medium sand (5 × 10^{-2} cm·s^{-1}), and even comparable to that of macropore soils such as loess (1 × 10^{-7}~2 × 10^{-3} cm·s^{-1}) [33].

Table 1. Porosity, water content, and permeability coefficient of Yellow River sediment.

Dry Bulk Density (g·cm^{-3})	Saturation Capacity (%)	Minimum Water Holding Capacity (%)	Degree of Saturation (%)	Void Ratio	Porosity (%)	Permeability Coefficient (cm·s^{-1})
1.60	40.64%	13.02%	51.24%	0.68	40.64%	2.91 × 10^{-3}

In the liquid-plastic limit joint determination test (Figure 4), the water content and penetration depth of the Yellow River sediment specimen were measured and plotted (Figure 4). The fitted line is $y = 1.559x - 22.955$. Calculations determined that the liquid limit (W_L) was 26.63%, the plastic limit (W_P) was 16.01%, and the plasticity index (I_P) was 9.62. These quantified limits reveal that the Yellow River sediment is a low liquid limit soil that is not readily susceptible to a fluid state.

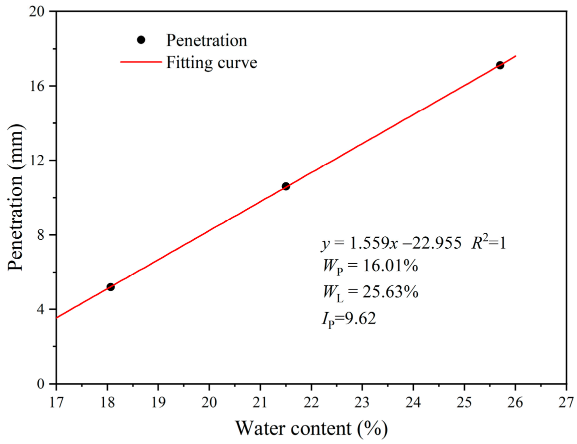

Figure 4. Relationship between 100 g cone depth and water content in the Yellow River sediment.

3.2. Mechanical Properties

3.2.1. Compaction Property

The results of the light compaction test, as shown in the graph (Figure 5), reflect the compaction and stability of the sediment used for filling and reclamation by measuring the dry density and number of compaction times at different water contents. The maximum dry densities for the three specimen groups range from 1.60 to 1.61 g·cm^{-3}, with an average of 1.61 g·cm^{-3}. This indicates that, under certain compaction conditions, the maximum dry density of the sediment is relatively stable, and does not change significantly with an increase in the number of compaction times. The corresponding optimal water content is between 16.58% and 17.08%, indicating that the sediment is most easily compressed to the maximum dry density of 1.61 g·cm^{-3} at around 17% water content.

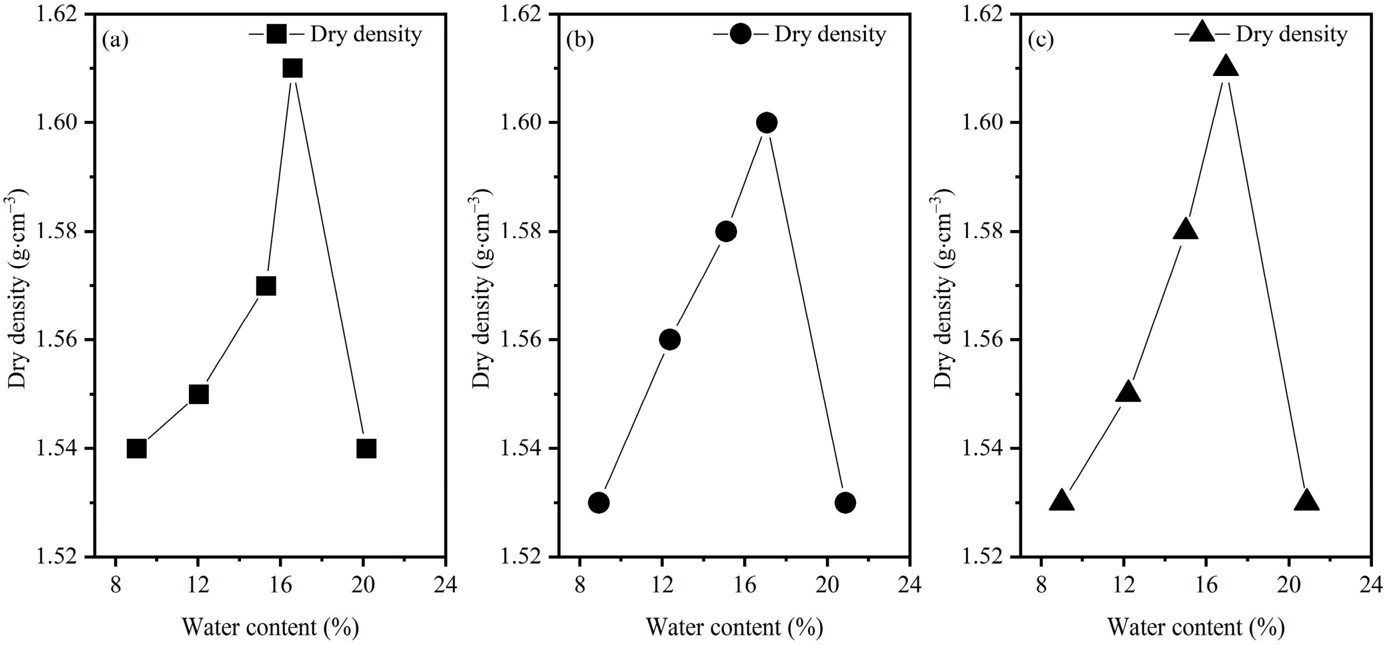

Figure 5. (**a**–**c**) Relationship between water content and dry density of Yellow River sediment.

3.2.2. Shear Strength

The shear stress–displacement curve (Figure 6) characterizes a compacted specimen of 1.60 g·cm^{-3} dry density under vertical stresses from 50 to 400 kPa. At this point, the shear stress increases with increasing shear displacement, but at a relatively slow rate. The shear stress can reach its peak within a shear displacement range of 4 to 6 mm, after which it tends to stabilize. The specimen reaches a certain state of stability, and the relationship between the shear stress and shear displacement becomes relatively stable, but still exhibits some fluctuations.

Based on the shear stress–horizontal displacement curves and strength curves of specimens from different particle size groups in the direct shear test, the maximum shear stress is taken as the shear strength S corresponding to the vertical stress, and a straight line is fitted to calculate the internal friction angle and cohesion of the particle size group. As can be seen from the figure (Figure 6), the fitted straight line is $y = 0.685x + 12.935$, for the specimen with dry bulk density of 1.60 g·cm^{-3}, the internal friction angle is 31.76°, and the shear strength is 12.935 kPa.

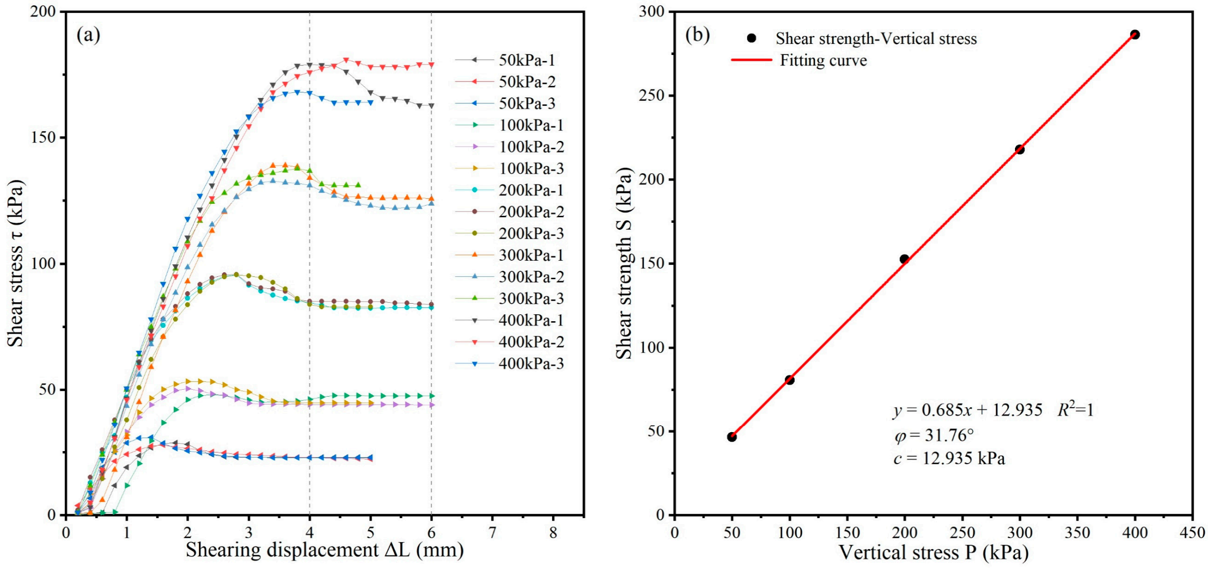

Figure 6. (**a**) The shear stress–horizontal displacement curves, (**b**) the shear strength envelopes.

3.2.3. Compressibility

The compression deformation curve (Figure 7) exhibits the deformation behavior of Yellow River sediment under vertical pressures of 12.5–400 kPa. The deformations are 0.08, 0.09, 0.13, 0.17, 0.22, and 0.35 mm at 12.5, 25, 50, 100, 200, and 400 kPa, respectively, indicating limited strain overall. Initially, the high deformation rate and steep curve signify rapid compression. After 50 kPa, the deformations increase progressively with higher vertical loading.

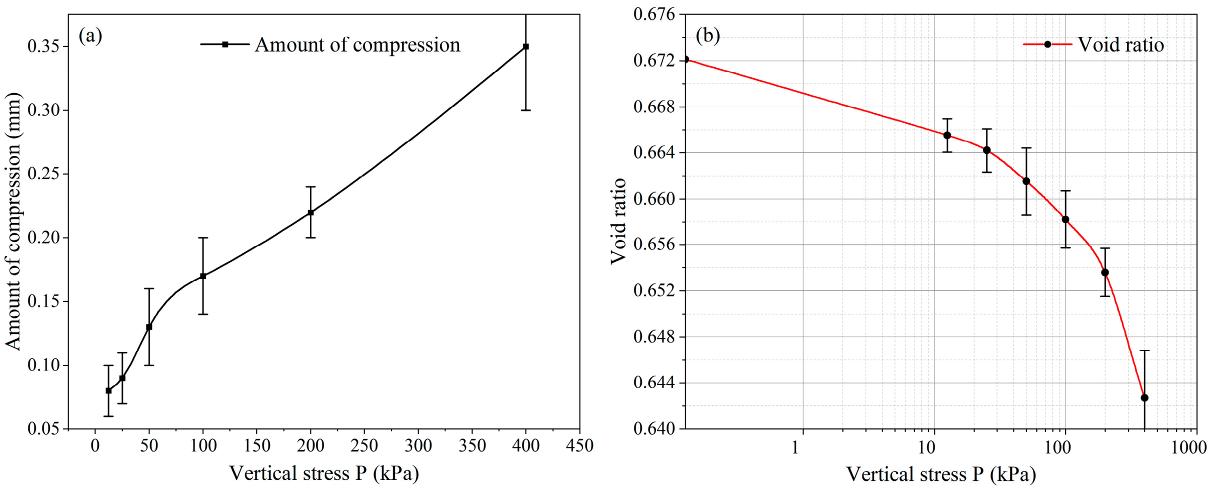

Figure 7. (**a**) Compression deformation curve and (**b**) semilogarithmic compression curve.

As can be seen from the figure (Figure 7), for the specimen with an initial water content of 17% and a dry density of 1.60 g·cm^{-3}, the void ratio is 0.672, with a point of maximum curvature. The initial segment has a small inclination, and as the pressure increases, the later segment of the curve drops sharply, and the porosity of the specimen gradually decreases. From 12.5 to 400 kPa, the porosity decreases from 0.666 to 0.643, with a small decrease of 3.43%.

The semilogarithmic compression curve (Figure 7) steepens with increasing pressure, indicating a significant decrease in the porosity of the specimen and higher compressibility, and vice versa. Generally, the compression coefficient $a_v = \frac{e_i - e_{i+1}}{p_{i+1} - p_i}$ MPa^{-1} is used to evaluate soil compressibility between 100 and 200 kPa pressure range [34]. Based on the figure, a_{1-2} is 0.05 MPa^{-1} , indicating that the soil has low compressibility. However, the compression coefficient increases from 0.03 MPa^{-1} between 25 and 100 kPa to 0.11 MPa^{-1} between 200 and 400 kPa. This pressure dependence shows higher compressibility at higher stresses.

In summary, combining the amount of compression and the semilogarithmic compression curve, the compression modulus $E_s = \frac{p_{i+1}-p_i}{(S_{i+1}-S_i)/1000}$ MPa^{-1} can be calculated at different axial pressures. The results show that as the axial pressure of Yellow River sediment increases from 12.5 to 400 kPa, the compression modulus also increases, which is 3.18, 15.63, 15.54, 25.53, 36.36, and 61.38 MPa^{-1}, respectively. This indicates that with the increase in pressure, Yellow River mud becomes more compact and the compressibility decreases.

4. Discussion

4.1. Causes of Productivity Barriers and Soil Reconstruction in Yellow River Sediment Reclamation

The grain size distribution of the filled and reclaimed Yellow River sediment shows a mean diameter (D_{50}) of 0.08 mm and a uniformity coefficient (C_u) of 1.75, indicating that the grains are fine, relatively uniform, and poorly graded. According to the soil classification used in engineering, the filled Yellow River sediment is made of fine sandy soil. According to the US Department of Agriculture soil texture classification standard, the sediment is sandy soil, close to the results of [35], with clay fractions of 3.54%, silt fractions of 9.80%, and sand fractions of 86.66%. The suspended matter in the Yellow River mainly comes from soil erosion of the Loess Plateau, and the suspended particles are fine [36]. There is less silt in the accumulated deposits in the dry channels, but more than 50% consists of fine sand particles of 0.1~0.05 mm [37]. Therefore, the overall permeability of 10^{-3} cm·s^{-1} is close to that of silty soil, making it feasible as a filling material for coal-mined subsided areas.

However, Yellow River sediments are nutrient deficient, with organic matter, total nitrogen, alkalyzable nitrogen, total potassium, extractable potassium, total phosphorus, and extractable phosphorus contents in the lower-middle, low, or very low range [25,35]. In order to remove productivity barriers as much as possible, the use of Yellow River sediments as fill material for reclamation needs to be improved through appropriate measures [15]. Soil reclamation can be achieved by mixing straw and topsoil [38]. In addition, in terms of physical and mechanical properties, the Yellow River sediment has an inhomogeneity coefficient of 1.75 and a curvature coefficient of 1.36, with more uniform particle sizes and poorer gradation, which is intuitively reflected by the fact that the reclaimed farmland is prone to the leakage of water and fertilizer compared with the control farmland. Zhenqi Hu [26] proposed the principle and method of sandwich-type soil reconstruction, and through the study of multiple profiles, Xiaotong Wang [27] found that the Yellow River sediment sandwich reclamation reduces seepage.

Therefore, the Yellow River sediment itself has poor physical and mechanical properties and productivity barriers, and in the process of reclaiming collapsed land, soil material mixing or the layered filling of original soil and Yellow River sediment is needed to ensure the quality of reclamation.

4.2. Causes and Criteria of Drainage Problems in Yellow River Sediment Reclamation

During the pipeline transport of Yellow River sediment for the filling reclamation of coal-mined subsided areas, the contained water needs to be drained to enable continuous and rapid construction. Drainage by sedimentation is an effective method [10,17,39]. However, in actual filling reclamation projects, the phenomenon of the water contained within the deeply filled Yellow River sediment not being drained draining after half a year of draining occurs.

There are two probable reasons for the ineffective drainage. First, based on the permeability coefficient of the reshaped Yellow River sediment, the constant head permeability test determined the permeability coefficient of the Yellow River sediment by sedimentation drainage to be 2.91 × 10^{-3} cm·s^{-1}, which is similar to the result of 4.39 × 10^{-3} cm·s^{-1} determined by [17], both in the same order of magnitude and differing by 1.5 times. This may be due to different filling densities and differences in grain sizes from dry channels and floodplains [15]. The permeability coefficient of the Yellow River sediment is similar to the results from variable head tests of actual specimens collected from the Yellow River's upstream floodplain, also in the same order of magnitude, generally between 1.33~2.51 × 10^{-3} cm·s^{-1} [40]. This indicates that the permeability of the filled and reclaimed Yellow River sediment is low, explaining the poor sedimentation drainage. Second, the subsided areas in eastern China have high groundwater levels around 1.5 m below the surface [7,41]. Therefore, slow drainage may also result from a lack of favorable hydraulic gradients, creating vertical and horizontal lateral seepage boundaries. Dredgers extracting Yellow River sediment from main channels also suck up viscous silt into the reclaimed areas. Another potential issue is that when the sand dredger extracts sediment from the dried channel of the Yellow River, the sticky mud is also drawn into the reclamation strips. Fine particles of silt and viscous particles of mud settle on the surface layer. On the one hand, the lower hydraulic conductivity of the viscous particle surface layer slows down the evaporation of water during the first stage, which is primarily governed by hydraulic conductivity. On the other hand, the finer capillary pores in the viscous particle surface layer also reduce the evaporation of water during the second stage, which is mainly driven by water diffusion [34]. When such sticky particles settle on the surface, they may form evaporation barriers within the filled Yellow River sediment section [42].

Consequently, the filled and reclaimed Yellow River sediment is still mostly sand particles. With proper drainage measures, the water can be drained. If good drainage measures can be implemented, given that the Yellow River sediment particles are fine and have a certain water holding capacity themselves, draining to 13% water content would be relatively quick and economical based on the minimum water holding capacity of the sediment.

4.3. Design Filled Ground Level for Reclamation: The Key to Controlling Subsidence

The compression coefficient of the Yellow River sediment (a_{1-2}) is 0.05 MPa^{-1}, indicating low compressibility soil. On the one hand, the sediment consists of rigid particles that are inherently difficult to compress, consistent with similar studies [43]; on the other hand, during the drainage of the Yellow River sediment, the simultaneous filling and draining process resembles dynamic consolidation, increasing pore water pressure in the sediment and decreasing effective stress, creating a quasi-overconsolidated state [44]. The recompacted sediment in the experiment exhibits overconsolidated soil characteristics.

It is clearly uneconomical to level the land using vertical pressure during construction. However, on the surface of the filled Yellow River sediment, a total thickness of 70 cm of topsoil and subsoil is needed to meet reclaimed land quality standards [45]. Therefore, the Yellow River sediment will gradually subside and deform under the self-weight stress of the overlying 70 cm of topsoil and subsoil layers. To ensure the design elevation post-deformation, a multi-layer sum method [34] constructs the compression model for layer i: $\Delta S_i = \frac{e_{1i} - e_{2i}}{1 + e_{1_i}} h_i$. Taking actual topsoil and subsoil thicknesses [45] and densities [27] of farmland reclamation as an example, the topsoil of 30 cm thickness and unit weight of 1.35 g·cm^{-3} produces a self-weight stress of 5.49 kPa, and the subsoil of 40 cm thickness and unit weight of 1.43 g·cm^{-3} produces a self-weight stress of 7.64 kPa. Thus, the total self-weight stress of the overlying soil is 13.13 kPa. Based on the compression curve, with the initial e_1 is 0.6721, taking 100 kPa added to the self-weight stress as a stable subsidence e_2 is 0.6576, the compression deformation ΔS_{100} is calculated. The natural subsidence deformation of the 100 cm Yellow River sediment is 0.87 cm (Table 2).

Table 2. Settlement of filling reclamation of topsoil, subsoil, Yellow River sediment under self-weight stress.

Soil Type	Thickness (cm)	Dry Bulk Density ($g{\cdot}cm^{-3}$)	Weight Density ($KN{\cdot}m^{-3}$)	Self-Weight Stress (kPa)	Settlement Deformation Amount (cm)
Topsoil	30	1.35	18.3	5.49	-
Subsoil	40	1.43	19.1	7.64	-
Yellow River sediment	100	1.60	20.8	20.8	0.87

The design elevation (H) and the backfill elevation (h) are important aspects of the Yellow River sediment reclamation land. The selection of these two parameters directly determines the quality and use value of reclaimed land. Because the goal of land reclamation is agricultural production, then the design elevation (H) needs to take into account the drainage, irrigation, and ploughing needs of the farmland. Clearly, as the backfill depth increases, the self-weight stress on the Yellow River sediment also changes accordingly. The sediment at different depths undergoes cumulative subsidence deformation over years due to repeated wetting and drying, resulting in corresponding subsidence. The design elevation (H) and backfill elevation (h) should subtract the accumulated subsidence and should satisfy the relationship: $\mathrm{h} - \sum_1^i \frac{e_{1i}-e_{2i}}{1+e_{1i}}\mathrm{h}_i = \mathrm{H}$.

4.4. Ensuring Construction Safety: Key Measures and Reference Standards

Generally, the internal friction angle increases with particle size [46]. The internal friction angle (φ) of the Yellow River sediment is 31.76°; refs. [47,48] also obtained similar results. Moreover, the internal friction angle differs significantly with different water contents [49]. Considering the water-laden sediment transported through pipelines that need to be dewatered before mechanical construction, the stress–strain and strength curves from direct shear tests at 9%, 13%, 17%, and 21% water content (Figure 8) show that with increased shear displacement, the shear stress gradually increases, slowing and stabilizing after 4–6 mm displacement. Increased vertical stress results in greater shear strength. This demonstrates that the axial load consolidates the specimen over a specific time interval with varying water contents. During the same time interval, the consolidation degree rises in correlation with higher vertical stress, which elevates the interaction force between particles and, in turn, enhances the shear resistance ability. To summarize, a higher water content reduces the friction angle and cohesion of the Yellow River sediment. The direct shear tests show that at a higher vertical stress, the shear resistance is higher due to more consolidation and particle interaction during the test period.

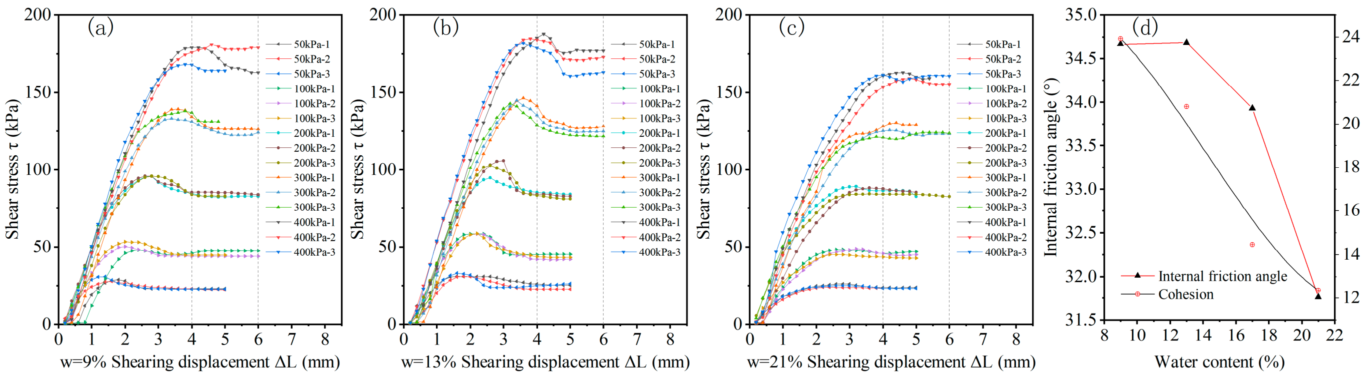

Figure 8. The shear stress–horizontal displacement curves and the shear strength envelopes. (**a**–**c**), and Figure 6 represent four treatments of water content; (**d**) the relationship between water content and internal friction angle.

For specimens with different water contents, the increased water content results in a reduction in friction angle. The angle decreased from 34.67° at a 9% water content to 31.76° at a 21% water content. Meanwhile, the cohesion remains relatively stable as water content increases from 9% to 13%, ranging from 23.92 to 20.79 kPa. However, when the water content surpassed 13%, the cohesion decreases sharply to between 14.46 and 12.36 kPa at water contents of 17% to 21%. This variation follows the characteristics of natural sand and is in accordance with the friction angles determined by the sediment measurements [47]. The field water content of 13.03% signifies that the sediment primarily comprises capillary water when the water content is less than 13%. When the water content exceeds 13%, the sediment particles saturate and reduce friction due to the lubrication effect of water [50]. Water plays the role of a lubricant since it lacks shear resistance, adheres to surfaces, and keeps contact points separate [51]. The capillary water between particles converges into curved menisci by surface tension, directing tension vectors toward contact surfaces. This provides the sediment with some cohesion. Friction between particles and cohesion between particles must be overcome for sediment particles to slip relative to each other [47].

To level the sediment safely and effectively during construction, it is necessary to prevent the construction equipment from sinking into it. The designed widths of the backfilled strips range from 15 to 20 m [17,52] for the three excavators made by Sany Heavy Machinery Limited. Medium and large excavators are the only ones with sufficient swing radii to avoid immersion. The medium excavator has a static contact pressure of 47.4 kPa. To support this pressure, the water content of the sediment must first be reduced below 17%. A design contact pressure of 56.88 kPa is obtained by applying a load factor of 1.2 to the dynamic load, and therefore, the water content must be kept below 9%. To accelerate reclamation progress, a backfilled strip width of around 12.5 m would require a small excavator model with a static contact pressure of 33 kPa and a design contact pressure of 39.6 kPa, allowing construction up to 21% water content (Table 3).

Table 3. Three types of Sany Heavy Machinery Limited excavator parameters and safety load.

Excavator Model	Tonnage (t)	Ground Specific Pressure (kPa)	Radius of Gyration (m)	Safe Load (kPa)
SY375H-S	big 30–50 t	68.8	10.875 m	82.56
SY205C	medium 13–30 t	47.4	10.28 m	56.88
SY75C	small 5–13 t	33	6.24 m	39.6

In summary, to avoid equipment immobilization, it is essential to reduce the water content. Lowering the water content is necessary for heavier equipment. Wider backfilled strips accommodate higher water content for a given size of equipment. The optimal solution is determined by optimizing the trade-off between productivity, equipment requirements, and material constraints.

4.5. Limitations and Future Works

This study explored the feasibility of using Yellow River sediments for coal-mined subsided land in the main canal of the Lower Yellow River from the perspective of physical and mechanical properties. It also provided valuable references for the challenges in construction such as drainage and elevation design. However, the physical and mechanical properties of Yellow River sediments may vary spatially, leading to differences in their behavior and impact on reclamation projects. This study might not fully capture the variability and heterogeneity of these sediments, thereby limiting the universality of the research results. Furthermore, this study might not have fully considered the complex interactions between Yellow River sediments and other environmental factors (such as groundwater, vegetation, and climate), which could significantly affect the reclamation process.

Therefore, in future studies, we will consider exploring the application of Upper Yellow River sediments in mining reclamation. For a more comprehensive understanding of the reclamation process, future studies could focus on the interactions between the Yellow River sediments and other environmental factors and their combined effects on land reclamation. Meanwhile, in order to better understand the long-term impacts of Yellow River sediments on the reclamation of coal-mined subsided land, future research could monitor and evaluate the long-term performance of reclaimed land. This will provide valuable information for optimizing reclamation strategies and managing reclaimed land sustainably.

5. Conclusions

To address these issues, this study discusses drainage and construction methods from the perspective of comprehending the physical and mechanical features of Yellow River sediment. This involves modifying the characteristics of the soil during the filling reclamation process. The conclusions of this study can be summarized as follows:

(1) The average particle size (D_{50}) of Yellow River sediment in coal-mined subsided land filling reclamation is 0.08 mm, which belongs to fine-grained sandy soil with a relatively uniform particle size and poor grading. After laboratory remolding and filling drainage, the dry capacity of Yellow River sediment is approximately 1.60 g·cm^{-3}. The minimum dry density is 1.37 g·cm^{-3}, and the maximum dry density is 1.83 g·cm^{-3}. The void ratio is 0.68, the porosity is 40.64%, the minimum water holding capacity is 13.02%, the saturation capacity is 40.64%, and the degree of saturation is 51.24%. The liquid limit (W_L) is 26.63%, the plastic limit (W_P) is 16.01%, and the plasticity index (I_P) is 9.62.

(2) The permeability of the Yellow River sediment used for reclaimed coal-mined subsided land is 2.91 $\times$ 10^{-3} cm·s^{-1}, which is similar to that of silt. Although this generally makes it suitable as a filling material for land reclamation purposes, its low permeability during drainage can create drainage obstacles during backfilling. In practical engineering projects, it is necessary to improve drainage measures to increase the construction rates. The permeability of the sediments similar to silt may cause drainage barriers during backfilling processes, which highlights the need for improving drainage systems and techniques to optimize filling and drainage efficiency.

(3) The Yellow River sediment used for reclaimed coal-mined subsided land exhibits internal friction angles that range from 34.67° to 31.76° and cohesions from 23.92 to 20.79 kPa. To ensure the safe levelling of the sediment during construction without submerging machinery, it is recommended that draining should achieve around 13% water content. At this level of water content, drainage can proceed swiftly while providing adequate stability for construction equipment operations. Achieving the appropriate water content allows maximum filling efficiency while simultaneously minimizing the risks of machinery immobilization during the levelling and compaction of the sediment. Further drainage might increase stability but could also extend the project schedule.

(4) The Yellow River sediment used for reclaimed coal-mined subsided land has a low compressibility compression coefficient of 0.05 MPa^{-1}. During reclamation construction, it would be uneconomical to undergo mechanical compression and compaction. With the increase in the depth of the backfill, the sediment experiences a change in overburden stress, which causes consecutive subsidence deformations over time because of wetting and drying cycles. Consider accounting for the cumulative subsidence by designing the final elevation (H) and initial backfill elevation (h) to comply with the equation: $\mathrm{h} - \sum_1^i \frac{e_{1i}-e_{2i}}{1+e_{1i}}\mathrm{h}_i = \mathrm{H}$.

Author Contributions: Conceptualization, Z.H. and H.S.; methodology, H.S.; software, H.S.; validation, S.W.; formal analysis, H.S.; investigation, H.S.; resources, H.S.; data curation, Z.H.; writing—original draft preparation, H.S.; writing—review and editing, Z.H.; visualization, S.W.; supervision, Z.H.; project administration, Z.H.; funding acquisition, Z.H. All authors have read and agreed to the published version of the manuscript.

Funding: This work was funded by the National Natural Science Foundation of China (No. 41771542).

Institutional Review Board Statement: Not applicable.

Informed Consent Statement: Not applicable.

Data Availability Statement: Data is contained within the article.

Acknowledgments: The authors would like to acknowledge the Experimental Management Center of the College of Geosciences and surveying engineering at China University of Mining and Technology-Beijing for their support and assistance with the experimental equipment for the mechanical properties of Yellow River sediment.

Conflicts of Interest: The authors declare that they have no known competing financial interests or personal relationships that could have appeared to influence the work reported in this paper.

References

1. Wu, Y.; Gao, X.; Zhou, D.; Zhou, R. Changes in Soil Physical and Chemical Properties after a Coal Mine Subsidence Event in a Semi-Arid Climate Region. *Pol. J. Environ. Stud.* **2022**, *31*, 2329–2340. [CrossRef] [PubMed]
2. Zheng, Q.; Wang, C.; Pang, L. Overburden and Surface Subsidence with Slicing Paste Filling Mining in Thick Coal Seams. *Front. Earth Sci.* **2023**, *10*, 1027816. [CrossRef]
3. Han, C.; Gao, Z.; Wu, Z.; Huang, J.; Liu, Z.; Zhang, L.; Zhang, G. Restoration of Damaged Ecosystems in Desert Steppe Open-Pit Coal Mines: Effects on Soil Nematode Communities and Functions. *Land Degrad. Dev.* **2021**, *32*, 4402–4416. [CrossRef]
4. Zeng, Y.; Pang, Z.; Wu, Q.; Hua, Z.; Lv, Y.; Wang, L.; Zhang, Y.; Du, X.; Liu, S. Study of Water-Controlled and Environmentally Friendly Coal Mining Models in an Ecologically Fragile Area of Northwest China. *Mine Water Environ.* **2022**, *41*, 802–816. [CrossRef]
5. Shang, H.; Zhan, H.-Z.; Ni, W.-K.; Liu, Y.; Gan, Z.-H.; Liu, S.-H. Surface Environmental Evolution Monitoring in Coal Mining Subsidence Area Based on Multi-Source Remote Sensing Data. *Front. Earth Sci.* **2022**, *10*, 790737. [CrossRef]
6. Kumar, D.; Singh, B. The Use of Coal Fly Ash in Sodic Soil Reclamation. *Land Degrad. Dev.* **2003**, *14*, 285–299. [CrossRef]
7. Wang, J.; Qin, Q.; Hu, S.; Wu, K. A Concrete Material with Waste Coal Gangue and Fly Ash Used for Farmland Drainage in High Groundwater Level Areas. *J. Clean. Prod.* **2016**, *112*, 631–638. [CrossRef]
8. Bai, D.-S.; Yang, X.; Lai, J.-L.; Wang, Y.-W.; Zhang, Y.; Luo, X.-G. In situ restoration of soil ecological function in a coal gangue reclamation area after 10 years of elm/poplar phytoremediation. *J. Environ. Manag.* **2022**, *305*, 114400. [CrossRef]
9. Xu, L.; Xu, S.; Yang, X.; Yan, J.; Meuser, H.; Makowsky, L. Study on Distribution Character of Physical and Chemical Properties and Heavy Metals in Reclaimed Land Filled with Fly Ash:A Case Study of Reclaimed Land of Luohe Power Plant in Huainan City. *J. Agro-Environ. Sci.* **2012**, *31*, 2352–2360.
10. Wang, P.; Shao, F.; Liu, J.; Li, X.; Hu, Z.S.; Yost, R. Simulated Experiment on Drainage and Fine Sediment Retention Effects of Geotextiles in Land Reclamation with Yellow River Sediments. *Trans. Chin. Soc. Agric. Eng.* **2015**, *31*, 72–80. [CrossRef]
11. Weber, J.; Straczynska, S.; Kocowicz, A.; Gilewska, M.; Bogacz, A.; Gwizdz, M.; Debicka, M. Properties of Soil Materials Derived from Fly Ash 11 Years after Revegetation of Post-Mining Excavation. *Catena* **2015**, *133*, 250–254. [CrossRef]
12. Wang, H.; Han, B.; Bian, Z. Simulation Research on Water Upright Movement in Reclaimed Soil by Filling. *J. China Univ. Min. Technol.* **2007**, *36*, 690–695.
13. Fu, J.; Lu, J.; Wu, M.; Ma, L.; An, C. Medium-Sized Channel Shaping in the Lower Yellow River Due to Water-Sediment Regulation. *Water Supply* **2023**, *23*, 192–205. [CrossRef]
14. Zhang, J.; Shang, Y.; Cui, M.; Luo, Q.; Zhang, R. Successful and Sustainable Governance of the Lower Yellow River, China: A Floodplain Utilization Approach for Balancing Ecological Conservation and Development. *Environ. Dev. Sustain.* **2022**, *24*, 3014–3038. [CrossRef]
15. Wang, P.; Hu, Z.; Shao, F.; Jiang, Z.; Qiao, Z.; Liu, D.; Chen, Y. Feasibility Analysis of Yellow River Sediment Used as the Filling Reclamation Material of Mining Subsidence Land. *J. China Coal Soc.* **2014**, *39*, 1133–1139. [CrossRef]
16. Hu, Z.; Shao, F.; Duo, L.; Wu, S.; Li, X.; McSweeney, K. Technique of Reclaiming Subsided Land with Yellow River Sediments in the Form of Spaced Strips. *J. China Coal Soc.* **2017**, *42*, 557–566. [CrossRef]
17. Wang, P. Technique of Filling and Drainage of Water-Sediment Mixture Used to Reclaim Mining Subsidence Land in Eastern China. Ph.D. Thesis, China University of Mining and Technology, Beijing, China, 2016.
18. Li, X.; Niu, W.; Zhang, W.; Wang, Y.; Wen, S.; Yang, X. Effect of Potassium Sulfate Fertilizer on Flocculation and Sedimentation of Static Yellow River Water. *J. Soil Water Conserv.* **2019**, *33*, 140–146+227. [CrossRef]

19. Zhao, R.; Hua, L.; Liu, H.; Yu, Y.; Song, Q.; Wu, S.; Yin, Y. Feasibility Study on Yellow River Sediment Used in Subgrade Filling of Expressway. *Yellow River* **2021**, *43*, 122–126. [CrossRef]
20. Yong-Gang, J.; Xiao-Lei, L.; Hong-Xian, S.; Jie-Wen, Z.; Su-Xia, H. The Effects of Hydrodynamic Conditions on Geotechnical Strength of the Sediment in Yellow River Delta. *Int. J. Sediment. Res.* **2011**, *26*, 318–330. [CrossRef]
21. Jing, X.; Li, G.; Zhang, Y.; Han, J.; Wang, B. Experimental Research on the Modification of the Yellow River Sediment. *Iran. J. Sci. Technol. Trans. Civ. Eng.* **2021**, *45*, 1031–1037. [CrossRef]
22. Jiang, S.; Xu, J.; Song, Y.; Xu, Y. Alkali-Activated Fly Ash Foam Concrete with Yellow River Silt: Physico-Mechanical and Structural Properties. *Constr. Build. Mater.* **2023**, *373*, 130879. [CrossRef]
23. Fang, L.; Li, C.; Chen, C.; Yan, G.; Zhang, Y.; Chai, X.; Zhang, Y. Research on Mechanical Performance of Yellow River Sediment Concrete in Kaifeng Section. *Yellow River* **2022**, *44*, 141–144+162. [CrossRef]
24. Mao, W.; Kang, S.; Wan, Y.; Sun, Y.; Li, X.; Wang, Y. Yellow River Sediment as a Soil Amendment for Amelioration of Saline Land in the Yellow River Delta. *Land Degrad. Dev.* **2016**, *27*, 1595–1602. [CrossRef]
25. Wang, P.; Hua, B.; Sun, H.; Fan, S.; Yang, Y.; Hu, Z. Investigation and Analysis of Obstacle Factors on Productivity of the Reclaimed Farmland Filled with Yellow River Sediment. *J. China Agric. Univ.* **2020**, *25*, 139–147. [CrossRef]
26. Hu, Z.; Duo, L.; Wang, X. Principle and Method of Reclaiming Subsidence Land with Inter-Layers of Filling Materals. *J. China Coal Soc.* **2018**, *43*, 198–206. [CrossRef]
27. Hu, Z.; Wang, X.; McSweeney, K.; Li, Y. Restoring Subsided Coal Mined Land to Farmland Using Optimized Placement of Yellow River Sediment to Amend Soil. *Land Degrad. Dev.* **2022**, *33*, 1029–1042. [CrossRef]
28. *GB-T50123-2019*; Standard for Geotechnical Testing Method. China Planning Press: Beijing, China, 2019.
29. *NY-T 1121.4-2006*; Soil Testing—Part 4: Method for Determination of Soil Bulk Density. China Agriculture Press: Beijing, China, 2006.
30. *SL 42-2010*; Technical Standard for Determination of Sediment Particle Size in Open Channels. Ministry of Water Resources of the People's Republic of China: Beijing, China, 2010.
31. *NY-T 1121.22-2010*; Soil Testing—Part 22: Cutting Ring Method for Determination of Field Water-Holding Capacity in Soil. China Agriculture Press: Beijing, China, 2010.
32. Swamee, P.K.; Ojha, C.S.P. Bed-Load and Suspended-Load Transport of Nonuniform Sediments. *J. Hydraul. Eng.* **1991**, *117*, 774–787. [CrossRef]
33. Mao, C. *Dikes Engineering Mannual*; China Water&Power Press: Beijing, China, 2009; ISBN 978-7-5084-6875-4.
34. Das, B.M. *Advanced Soil Mechanics*, 5th ed.; CRC Press: Boca Raton, FL, USA; Taylor & Francis Group: Abingdon, UK, 2019; ISBN 978-1-351-21516-9.
35. Wang, X. Mechanism of Action of Interlayers in Reconstructed Soil Filled with Yellow River Sediments and Its Simulation. Ph.D. Dissertation, China University of Mining and Technology, Beijing, China, 2020.
36. Van Maren, D.S.; Winterwerp, J.C.; Wang, Z.Y.; Pu, Q. Suspended Sediment Dynamics and Morphodynamics in the Yellow River, China. *Sedimentology* **2009**, *56*, 785–806. [CrossRef]
37. Zhou, J.; Zhang, M. Coarse Sediment and Lower Yellow River Siltation. *J. Hydro-Environ. Res.* **2012**, *6*, 267–273. [CrossRef]
38. Bednik, M.; Medyńska-Juraszek, A.; Dudek, M.; Kloc, S.; Kręt, A.; Łabaz, B.; Waroszewski, J. Wheat Straw Biochar and NPK Fertilization Efficiency in Sandy Soil Reclamation. *Agronomy* **2020**, *10*, 496. [CrossRef]
39. Shao, F.; Wang, P.; Li, E.; Jiang, Z.; Qiao, Z.; Liu, D.; Chen, Y. The Feasibility of Application of Desilting and Drainage Engineering Measures in the Process of Filling Reclamation with Yellow River Sediment. *Energy Environ. Prot.* **2013**, *27*, 1–5.
40. Wang, Q.; Xie, J.; Yang, J.; Liu, P.; Chang, D.; Xu, W. Research on Permeability Coefficient of Fine Sediments in Debris-Flow Gullies, Southwestern China. *Soil Syst.* **2022**, *6*, 29. [CrossRef]
41. He, T.; Xiao, W.; Zhao, Y.; Chen, W.; Deng, X.; Zhang, J. Continues Monitoring of Subsidence Water in Mining Area from the Eastern Plain in China from 1986 to 2018 Using Landsat Imagery and Google Earth Engine. *J. Clean. Prod.* **2021**, *279*, 123610. [CrossRef]
42. Lehmann, P.; Merlin, O.; Gentine, P.; Or, D. Soil Texture Effects on Surface Resistance to Bare-Soil Evaporation. *Geophys. Res. Lett.* **2018**, *45*, 10398–10405. [CrossRef]
43. Jie, L.; Ping, L.; Xiao, L.; Yuanqin, X.; Wei, G. The Characteristics of Consolidation Settlement and Its Contribution to the Topographical Change in the Northern Modern Huanghe River Subaqueous Delta in China. *Acta Oceanol. Sin.* **2015**, *34*, 136–142. [CrossRef]
44. Yang, X.; Jia, Y.; Liu, H.; Shan, H. Research on consolidation characteristics and origin of the yellow river estuary sediments. *Mar. Geol. Quat. Geol.* **2009**, *29*, 29–34.
45. Hu, Z.; Duo, L.; Shao, F. Optimal Thickness of Soil Cover for Reclaiming Subsided Land with Yellow River Sediments. *Sustainability* **2018**, *10*, 3853. [CrossRef]
46. Alias, R.; Kasa, A.; Taha, M.R. Particle Size Effect on Shear Strength of Granular Materials in Direct Shear Test. *Int. J. Civ. Environ. Eng.* **2014**, *8*, 1144–1147.
47. Fan, Z.; Qu, J.; Zhou, H. The Relationship between Sand Particle Internal Friction Angle and Particle Size, Water Content and Slope Angle. *J. Desert Res.* **2015**, *35*, 301–305. [CrossRef]
48. Yang, Z.; Liu, X.; Su, X.; Guo, L.; Cui, Y.; Jia, C.; Ling, X. CPT-Based Evaluation of Sediment Characteristics and Effective Internal Friction Angle in the Yellow River Estuary. *Mar. Georesour. Geotechnol.* **2022**, *40*, 1108–1118. [CrossRef]

49. Gu, T.; Wang, J.; Wang, C.; Bi, Y.; Guo, Q.; Liu, Y. Experimental Study of the Shear Strength of Soil from the Heifangtai Platform of the Loess Plateau of China. *J. Soils Sediments* **2019**, *19*, 3463–3475. [CrossRef]
50. Canakci, H.; Hamed, M.; Celik, F.; Sidik, W.; Eviz, F. Friction Characteristics of Organic Soil with Construction Materials. *Soils Found.* **2016**, *56*, 965–972. [CrossRef]
51. Xing, H.; Liu, J.; Wang, L.; Yao, X.; Wang, C.; Zhang, Y.; Zhou, D. Friction Characteristics of Soil-Soil Interface and Root-Soil Interface of Caragana Intermedia and Salix Psammophila. *Tribology* **2010**, *30*, 87–91. [CrossRef]
52. Duo, L. Key Technologies of Subsidence Land Reclamation Filled with Yellow River Sediments by Alternating Mutli-Times and Multilayers. Ph.D. Thesis, China University of Mining and Technology, Beijing, China, 2019.